Pubblicazioni del Centro De Giorgi
Proceedings of the Interdisciplinary Workshop on Mathematical Methods in Biomedical Imaging and Intensity-Modulated Radiation Therapy (IMRT), Pisa, Italy, October 2007.

INVERSE TRANSPORT FROM ANGULARLY AVERAGED MEASUREMENTS AND TIME HARMONIC ISOTROPIC SOURCES

Guillaume Bal

ABSTRACT. We summarize recent results obtained on the unique identifiability of constitutive parameters in transport equations from angularly averaged measurements and isotropic sources. Such settings, which are accurate frameworks in many applications of transport equations, result in severely ill-posed inverse problems. One possibility to improve the reconstructions is then to use time harmonic sources (frequency modulations). We show that frequency modulations of the radiating sources allow us to better reconstruct the optical parameters in a transport equation and provide theoretical explanations as to why this is the case.

1. Introduction

The transport equation models the (phase-space) density of particles $u(x,v)$ at position x propagating with direction v. The transport equation of interest in this paper is as follows:

$$\begin{aligned} &i\omega u + v\cdot\nabla_{\mathbf{x}} u + \sigma(x)u = \int_{S^{n-1}} k(x,v'\cdot v)u(x,v')d\mu(v'), && \text{in } D\times S^{n-1}\\ &u(x,v) = f(x,v) && \text{on } \Gamma_-, \end{aligned} \tag{1.1}$$

where D is an open, convex, bounded, subset in $\mathbb{R}^n$, n is spatial dimension, S^{n-1} is the unit sphere in $\mathbb{R}^n$ with Lebesgue measure $d\mu(v)$,

Key words and phrases. inverse transport, angularly averaged measurements, isotropic sources, time-harmonic sources.

The author was supported in part by NSF Grants DMS-0239097 and DMS-0554097.

$\Gamma_\pm = \{(x,v) \in \partial D \times S^{n-1}, \pm v \cdot \nu(x) > 0\}$, $\nu(x)$ outward normal to D at $x \in \partial D$. ω is the modulation frequency (divided by light speed c), corresponding to time-harmonic boundary sources of the form $e^{i\omega t} f(x,v)$. The optical parameters are $\sigma(x)$, the total absorption parameter, and $k(x,\kappa)$, the scattering coefficient. In many applications, $k(x,\kappa)$ may be written as $k(x)\phi(\kappa)$, where $\phi(\kappa)$ measures the degree of anisotropy.

Existence theories for the transport equation (1.1) are well-developed. We refer the reader to e.g. [**5, 8**]. Under appropriate sub-criticality assumptions -for instance by imposing that scattering is not larger than total absorption-, we obtain the existence of a solution $u(x,v) \in L^1(D \times S^{n-1})$ provided that $f(x,v) \in L^1(\Gamma_-, \tau d\xi)$, where $\tau(x,v)$ is the maximal distance from x to ∂D in direction $\pm v$ and where we have defined $d\xi = |v \cdot \nu(x)| d\mu(v) dS(x)$ with dS the (Lebesgue) measure on ∂D. Moreover, the restriction to the outgoing solution at the domain's boundary $u_{|\Gamma_+}(x,v)$ for $x \in \partial D$ and $v \cdot \nu(x) > 0$ belongs to the space $L^1(\Gamma_+, \tau d\xi)$.

Let us assume for now that $\omega = 0$. The inverse transport problem consists of reconstructing the optical parameters $\sigma(x)$ and $k(x,\kappa)$ (or more generally $k(x,v',v)$) from boundary measurements. The most general boundary measurements available consist of full knowledge of the albedo operator:

$$\mathcal{A} : u_{|\Gamma_-} \mapsto u_{\Gamma_+},$$

where $u(x,v)$ is the solution to (1.1) with boundary conditions $f = u_{|\Gamma_-}$ on Γ_-. In dimension $n \geq 2$, the albedo operator uniquely determines $\sigma(x)$ and in dimension $n \geq 3$, the albedo operator uniquely determines $k(x,v',v)$. In dimension $n = 2$, $k(x,v',v)$ is uniquely determined when it is sufficiently small. We refer the reader to [**12**] for a review of available theory and stability results when the full albedo operator is known. The uniqueness results are based on the following observation. The ballistic component in $\mathcal{A}$, corresponding to setting $k = 0$ in (1.1), is always more singular than the rest of the albedo operator. This contribution allows us to invert $\sigma(x)$ by inverse X-ray transform. In dimension $n \geq 3$, the single scattering component in $\mathcal{A}$, i.e., the component of $\mathcal{A}$ that is linear in k, is still more singular than the components in $\mathcal{A}$ that are at least quadratic in k. Such a component then allows us to reconstruct $k(x,v',v)$ explicitly once σ is known.

In practice, however, the full albedo operator is rarely available, either because particle counts would be too low to allow for a good resolution in the angular variable, or because sampling the $4(n-1)$ dimensions

of the albedo operator would be too time consuming. This paper reviews recent results obtained in cases where the measurements are much more restrictive.

A typical available measurement at a domain's boundary is the current of particles, defined as

$$J(x) = \int_{S^{n-1}} v \cdot \nu(x) u(x,v) d\mu(v), \quad x \in \partial D. \tag{1.2}$$

This current may be separated as the part where $v \cdot \nu(x) < 0$, which involves only the known boundary conditions, and the part where $v \cdot \nu(x) > 0$, which corresponds to the outgoing flux of particles that is measured in practice. Current measurements also correspond to the measurements available in inverse transport problems with highly scattering media. Indeed, in such a situation, the solution $U(x)$ to a diffusion equation becomes a good approximation to the transport solution $u(x,v)$ of (1.1) and $u(x,v) \approx U(x) - \frac{1}{\sigma} v \cdot \nabla U$, so that $J(x) \approx D \frac{\partial U}{\partial \nu}$ with $D = \frac{1}{d\sigma}$. We refer the reader to e.g. [**5**] for the validity of the diffusion approximation and to e.g. [**1**] for applications of inverse transport in highly scattering media to optical tomography.

The question now is to know whether the optical parameters may be reconstructed from angularly averaged measurements given by $J(x)$ or by other angular integrals where $v \cdot \nu(x)$ is replaced by a more general, known, kernel $m(x,v)$. In the case where the source term $f(x,v)$ is still allowed to depend on the angular variable, the answer is that $\sigma(x)$ is uniquely determined and that $k(x)$ is uniquely determined under appropriate analyticity constraints on the coefficients; we refer the reader to [**7**] for more details and related stability estimates. Because $f(x,v)$ is still allowed to be singular in the whole phase space $D \times S^{n-1}$, the ballistic component of the measurements (corresponding to $k = 0$) is more singular than the other contributions to the measurements and thus allows us to reconstruct $\sigma(x)$ by inverse X-ray transform as in the case of full knowledge of $\mathcal{A}$.

The most restrictive measurements are of the form $f(x,v) = f(x)$, where the incoming radiation is independent of the angular variable. Because of their close relationship with inverse theories for the diffusion equation, we call diffusion-type measurements the following type of measurements

$$\mathcal{D} : f(x) \mapsto J(x), \tag{1.3}$$

where u solves (1.1) with $f = f(x)$ as boundary conditions and $J(x)$ is defined in (1.2). In diffusion theory, $\mathcal{D}$ would correspond to the Dirichlet

to Neumann map, which uniquely determines a scalar valued diffusion coefficient [**13**].

The theory of the reconstruction of optical parameters from knowledge of $\mathcal{D}$ is still in its infancy. In section 2, we present recent results obtained in [**3**] on the reconstruction of $k(x)$ under strong assumptions: $\sigma(x)$ is known and both $k(x)$ and $\sigma(x)$ are small. These results show that we can reconstruct the low-frequency component of $k(x)$ with an error proportional to the high-frequency component of $k(x)$. The method of inversion is surprisingly similar to the linearization of the inverse diffusion problem, the so-called Calderón problem [**4**]. The same complex geometrical optics (CGO) solutions are used. The practical downside of such an analogy is that the stability estimates for the reconstruction of the scattering coefficient are of exponential type: high frequency components in the data are exponentially amplified during the reconstruction, which makes the inversion a severely ill-posed problem.

One of the major differences between full angular measurements as in $\mathcal{A}$ and angularly averaged measurements as in $\mathcal{D}$ is that $\mathcal{A}$ has singular components that are no longer present in $\mathcal{D}$. Mathematically, this implies that Hölder-type stability results available from angularly resolved measurements are replaced by exponential type stability results. Mildly ill-posed problems become severely ill-posed problem, and thus the number of degrees of freedom one can reasonably expect to reconstruct from available data will be much smaller in the latter case.

An interesting possibility to improve the reconstruction capabilities of optical parameters from angularly averaged measurements, which are often all that is available in practice, is to use modulated frequencies, i.e., $\omega \neq 0$ in (1.1). It is known in diffusion theory that $\omega \neq 0$ is necessary to reconstruct both the diffusion coefficient and the absorption coefficient $\sigma_a(x) = \sigma(x) - \int_{S^{n-1}} k(x, v \cdot v') d\mu(v')$. In transport theory with angularly averaged measurements, the same conclusion is expected to hold: we expect to obtain better reconstructions for $\sigma(x)$ and $k(x)$ when $\omega \neq 0$. This was observed numerically in [**10, 11**]. The salient features of these two works that are of interest in this paper are recalled in section 3. The main results are that inverse transport reconstructions from knowledge of $\mathcal{D}^\omega$, the equivalent of (1.3) for values of $\omega \neq 0$, perform significantly better when the modulation frequency ω is a large fraction of a GHz than when $\omega = 0$. Moreover, the cross-talk between the reconstructions of the absorption and scattering coefficients (the phantom reconstruction of a scattering fluctuation if the presence of an absorbing-only fluctuation and vice-versa) is significantly reduced when ω increases.

In order to explain these two behaviors, namely that reconstructions are better and cross-talk is reduced when larger frequency modulations ω are being used, we consider the asymptotic regime of very high modulations ω. It turns out that the transport solution $u(x, v; \omega)$ of (1.1) admits the following asymptotic expansion in two dimensions of space. The ballistic component, which corresponds to solving (1.1) with $k = 0$, has an intensity independent of ω. Its phase is modified by $e^{i\omega l}$, where l is the distance between the source and the detector. Because scattering can occur over the whole domain D, the single scattering term is of order $\frac{1}{\sqrt{\omega}}$. The reason is that signals arrive with a phase equal to $e^{i\omega(l_1+l_2)}$, where l_1 is the distance from the source to the location of the scattering and l_2 the distance from the location of the scattering to the detector. The phase shift $l_1 + l_2$ depends on position so that signals arrive at the detector with different phases that interfere destructively. Double scattering and higher contributions provide a term much smaller than $\frac{1}{\sqrt{\omega}}$. This allows us to reconstruct $\sigma(x)$ and $k(x)\phi(0)$ (scattering in the forward direction) from knowledge of $\mathcal{D}^{\omega_1}$ and $\mathcal{D}^{\omega_2}$ for $\omega_1 \neq \omega_2$ sufficiently large. The reconstruction is based on the inversion of a classical Radon transform for the attenuation σ and a weighted Radon transform for the scattering coefficient $k(x)$. This means that the reconstruction of the optical coefficients from angularly averaged measurements and isotropic sources becomes a mildly ill-posed problem in the limit of infinitely large modulation frequencies. More details on the derivation are provided in section 4.

The theory, although valid for sufficiently large modulation frequencies, gives a reasonable intuition as to why the reconstructions in [**10, 11**] performed better for high values of ω than for continuous waves, where $\omega = 0$. The theory also indicates that higher values of the modulation frequency would allow us to obtain sharper reconstructions of the optical parameters provided that the phase modulations can be measured accurately. The main parameter that allows us to gauge the validity of the high modulation regime is the total phase shift $p_s = \frac{2\pi\omega l}{c}$ as particles travel across the domain. The decorrelation of scattering events will occur provided that p_s is sufficiently large, say on the order of 5. For a domain of size $l = 10$cm, this corresponds to $\omega = \frac{2\pi 5c}{l} \approx 300c \approx 100$GHz. Such frequencies are 100 times what is currently being used in practice in optical tomography, and may therefore be out of reach at least in the near future.

2. Reconstructions from diffusion-type measurements

We summarize here results obtained in [**3**]. Let $f(x)$ be the incoming boundary conditions and $u(x,v)$ the solution in (1.1). Let then $g(x)$ be a test function defined on ∂D. We define the measurements

$$\mathcal{M}(f,g)=\int_{\partial D} g(x)J(x)dS(x)=\int_{\partial D} g(x)\mathcal{D}f(x)dS(x), \qquad (2.1)$$

where J is defined in (1.2) and $\mathcal{D}$ in (1.3). Under fairly restrictive assumptions, including that $\sigma(x)$ is assumed to be known, we show that the low-frequency part of $k(x)$ may be reconstructed from knowledge of $\mathcal{M}(f,g)$ for all (f,g) in $L^1(\partial D)$.

The reconstructions are based on the following decomposition of the measurement operator:

$$\mathcal{M}(f,g)=\langle f\otimes g, T_0\rangle_{L^2((\partial D)^2)}+\sum_{m=1}^{\infty}\langle f\otimes g, T_m(k)\rangle_{L^2((\partial D)^2)}, \quad (2.2)$$

with the notation $\langle f\otimes g, T\rangle = \int_{(\partial D)^2}\bar{T}(x,y)f(x)g(y)dS(x)dS(y)$, where $\bar{T}$ is complex conjugation of T. Here, T_0 corresponds to the ballistic part of the measurements obtained by setting $k=0$ in (1.1). The kernels $T_m(k)$ are then multilinear of order m in $k(x)$ so that $T_1(k)$ corresponds to single scattering, $T_2(k)$ double scattering, and so on.

More precisely, let us define

$$E(x,y)=\exp\left(-\int_0^{|y-x|}\sigma\Big(x+\frac{y-x}{|y-x|}s\Big)ds\right), \qquad (2.3)$$

the total attenuation between points x and y and by induction

$$E(x_1,\ldots,x_{n-1},x_n)=E(x_1,\ldots,x_{n-1})E(x_{n-1},x_n), \qquad (2.4)$$

the total attenuation on the broken path $[x_1,\ldots,x_n]$. Then we have

$$\begin{aligned} T_0(x_0,x) &= \frac{E(x_0,x)|\nu_x\cdot v||\nu_{x_0}\cdot v|}{|x_0-x|^{n-1}},\\ T_m(k)(x_0,x) &= \int_{D^m} k(x_1)\cdots k(x_m)\frac{E(x_0,\ldots,x_m,x)}{|x_0-x_1|^{n-1}\cdots|x_m-x|^{n-1}}\\ &\qquad\times|\nu_{x_0}\cdot v_0||\nu_x\cdot v_m|dx_1\ldots dx_m. \end{aligned} \qquad (2.5)$$

Note that T_0 and $T_m(k)$, taken at points x and x_0, are the measurements given source $f=\delta_{\{x_0\}}$, and weight $g=\delta_{\{x\}}$, where $\delta_{\{x\}}$ is the surface delta function such that $\int_{\partial D}\delta_{\{x\}}f(y)dS(y)=f(x)$. In other words

$\sum_{m=0}^{\infty} T_m(k)(x_0,x)$ is formally the Schwartz kernel of the operator $\mathcal{D}$:

$$\mathcal{D}f(x) = \int_{\partial D} \Big(T_0(x_0,x) f(x_0) + \sum_{m=1}^{\infty} T_m(k)(x_0,x) f(x_0) \Big) dx_0. \quad (2.6)$$

We refer the reader to [**3**] for the derivation of (2.2), which relies on writing the solution to (1.1) in integral form; see e.g. [**5, 8**].

Because $\sigma(x)$ is known, then so is $\langle f \otimes g, T_0 \rangle$ in (2.2). For k sufficiently small, $\mathcal{M}(f,g) - \langle f \otimes g, T_0 \rangle$ is then equal to $\langle f \otimes g, T_1(k) \rangle$ up to a small term that is quadratic in k. The first objective is therefore to reconstruct k from the linearized measurements $\langle f \otimes g, T_1(k) \rangle$. This may be done explicitly when σ vanishes. Specifically, we have that

$$\langle f \otimes g, T_1(k) \rangle_{L^2((\partial D)^2)} = \langle Af\, Ag, k \rangle_{L^2(D)},$$

where the so-called half-adjoint operator A is defined as

$$Af(y) = \omega_n \int_{\partial D} f(x) E(x,y) \partial_{\nu_x} N(x,y)\, d\mu(x). \quad (2.7)$$

Here ω_n is the measure of the unit sphere S^{n-1} and $N(x,y) = N(x-y)$ is the Newton potential

$$N(x,y) := \frac{1}{c_n |x-y|^{n-2}} \ \ (n>2); \qquad \frac{1}{c_2} \log|x-y| \ \ (n=2),$$

where $c_n = (2-n)\omega_n$ and $c_2 = 2\pi$. Indeed, we verify that $\partial_{\nu_x} N(x,y) = \frac{\nu_x \cdot (x-y)}{\omega_n |x-y|^n}$. Let A_0 be the operator defined as A in (2.7) with $\sigma = 0$ so that $E(x,y) \equiv 1$. We thus draw the following conclusion: $A_0 f(y)$ is a *harmonic* function on D because $y \mapsto N(x,y)$ is. Moreover, each sufficiently smooth harmonic function v on D may be constructed as $v = A_0 f_v$ for some function f_v on ∂D. The implicit construction goes as follows. Let us define

$$\mathscr{A}_0 f(y) = \omega_n \int_{\partial D} f(x) \partial_{\nu_x} N(x,y)\, d\mu(x),$$

the classical double layer potential for $y \in \partial D$. It is a classical result that $\frac{1}{2} I + \omega_n^{-1} \mathscr{A}_0$ is an isomorphism on $L^2(\partial D)$. We may then define the operator

$$A_0^{\dagger} u := (\frac{1}{2} I + \omega_n^{-1} \mathscr{A}_0)^{-1} (\omega_n^{-1} u|_{\partial D}), \quad (2.8)$$

and verify that $A_0 A_0^{\dagger} u = u|_D$ for all harmonic function $u \in H^{\frac{1}{2}}(D)$.

We are now ready to use the same Complex Geometrical Optics (CGO) solutions as in the Calderón problem [**4**]. Let $\mathbb{C}^n \ni \rho = \frac{1}{2}(\xi + i\eta)$,

where $\xi, \eta \in \mathbb{R}^n$, $\xi \cdot \eta = \sum_{i=1}^n \xi_i \eta_i = 0$, and $|\xi| = |\eta|$. Then the functions $e^{i\rho\cdot x}$, and $e^{i\bar\rho\cdot x}$ are harmonic, and $e^{i\rho\cdot x}e^{i\bar\rho\cdot x} = e^{i\xi\cdot x}$. Define the boundary conditions

$$f_\xi(x) := A_0^\dagger e^{-i\rho\cdot x} \text{ and } g_\xi(x) := A_0^\dagger e^{-i\bar\rho\cdot x}, \quad x \in \partial D. \tag{2.9}$$

Then we find that

$$\begin{aligned} \langle f_\xi \otimes g_\xi, T_1^0(k)\rangle_{L^2((\partial D)^2)} &= \langle A_0 f_\xi\, A_0 g_\xi, k\rangle_{L^2(D)} \\ &= \langle e^{-i(\xi,\cdot)}, k\rangle_{L^2(D)} \\ &:= \hat k(\xi), \end{aligned} \tag{2.10}$$

where $T_1^0(k)$ is defined as $T_1(k)$ with $\sigma = 0$, whence $E \equiv 1$.

In other words, we obtain an explicit reconstruction of $\hat k(\xi)$ from the single scattering measurements provided that absorption $\sigma \equiv 0$. We have thus two sources of error: one is from the higher scattering contributions $T_m(k)$ for $m \geq 2$, and one is from the error coming from the non-zero absorption $T_1^\sigma(k) := T_1(k) - T_1^0(k)$. The approximation $\hat k_l(\xi)$ of $\hat k(\xi)$ obtained by this linearization algorithm is thus given by

$$\begin{aligned} \hat k_l(\xi) &= \mathcal{M}(f_\xi, g_\xi) \\ &= \hat k(\xi) + \langle f_\xi \otimes g_\xi, T_1^\sigma(k)\rangle + \sum_{m=2}^\infty \langle f_\xi \otimes g_\xi, T_m(k)\rangle. \end{aligned} \tag{2.11}$$

The error made by the linearization is given by

$$|\hat k_l(\xi) - \hat k(\xi)| \leq \Big(\|T_1^\sigma(k)\|_{L^2} + \sum_{m\geq 2} \|T_m(k)\|_{L^2}\Big)\|f_\xi\|_{L^2}\|g_\xi\|_{L^2}. \tag{2.12}$$

Under smallness assumptions on k and σ, we obtain that

$$\|T_1^\sigma(k)\|_{L^2} \leq C\|\sigma\|_\infty \|k\|_\infty, \quad \sum_{m\geq 2} \|T_m(k)\|_{L^2} \leq C\|k\|_\infty^2.$$

The bound on $\|f_\xi\|_{L^2}$ and $\|g_\xi\|_{L^2}$ is however exponentially large as ξ increases:

$$\|f_\xi\|_{L^2(\partial D)}, \|g_\xi\|_{L^2(\partial D)} \leq Ce^{\alpha|\xi|}, \qquad \alpha = \frac{\text{diam}(D)}{2}. \tag{2.13}$$

for some constant C independent of ξ. This shows that

$$|\hat k_l(\xi) - \hat k(\xi)| \leq C\|k\|_\infty(\|\sigma\|_\infty + \|k\|_\infty)e^{2\alpha|\xi|}. \tag{2.14}$$

Errors on the reconstructions of the Fourier modes of $k(x)$ grow exponentially with wavenumber ξ. The reconstruction of $k(x)$ is severely ill-posed.

Because the operator T_1^0 (defined as the integral operator with Schwartz kernel $T_0^1(x,y)$) is highly smoothing, which is responsible for the above

severe ill-posedness, we introduce the following approximate inverse. Let $\chi(\xi)$ be a compactly supported (to simplify) smooth function in $\mathbb{R}^n$. Typically $\chi(\xi) = 1$ for $|\xi| < M$ and $\chi(\xi) = 0$ for $|\xi| > M$ if one wants to reconstruct all frequencies $|\xi| < M$ of $k(x)$. Let then $P_\chi k$ be the operator

$$P_\chi k := \int_{\mathbb{R}^n} \hat{k}(\xi)\chi(\xi)e^{i\xi\cdot x}\,\frac{d\xi}{(2\pi)^n},$$

and let $k_\chi = P_\chi k$. We define

$$T^\chi h(x) := \int_{\mathbb{R}^n} \langle f_\xi \otimes g_\xi, h\rangle_{L^2((\partial D)^2)}\chi(\xi)e^{i\xi\cdot x}\,\frac{d\xi}{(2\pi)^n}, \tag{2.15}$$

as the regularized inverse of T_1^0 (since $T^\chi T_1^0 = P_\chi$). Using (2.12), we find that

$$\|T^\chi\|_{L^2\to L^\infty} \le C\|\chi(\xi)e^{2\alpha|\xi|}\|_{L^1(\mathbb{R}^n)},$$

so that eventually,

$$\|k_\chi(x) - P_\chi k_l(x)\|_\infty \le C\|k\|_\infty(\|\sigma\|_\infty + \|k\|_\infty)\|\chi(\xi)e^{2\alpha|\xi|}\|_{L^1(\mathbb{R}^n)}, \tag{2.16}$$

where $P_\chi k_l(x)$ is the regularized inverse Fourier transform of $\hat{k}_k(\xi)$ defined in (2.11).

We obtain an error estimate for the low-frequency component of $k(x)$. Note however that the estimate is very large, even for small values of ξ, unless σ and k are extremely small. Such an estimate may be improved by using an iterative scheme. Once $P_\chi k_l(x)$ has been obtained, it may be used to estimate the error term in (2.11), which may be used to modify the measured data $\mathcal{M}(f,g)$ and use the linearized inverse one more time to obtain a better estimate of $k_\chi(x)$. More precisely, let us define iteratively:

$$\begin{aligned} k_\chi^0 &= T^\chi \sum_{m=1}^{\infty} T_m(k) \\ k_\chi^{\nu+1} &= T^\chi\left(\textstyle\sum_{m=1}^{\infty} T_m(k)\right) - T^\chi\left(T_1^\sigma(k_\chi^\nu) + \sum_{m=2}^{\infty} T_m(k_\chi^\nu)\right). \end{aligned} \tag{2.17}$$

Here, $T_m(k)$ are seen as integral operators with Schwartz kernel $T_m(k)(x,y)$. Note that $k_\chi^0 = P_\chi k_l$, the linearized reconstruction. Under appropriate smallness conditions on σ and k, which are given explicitly in [**3**], a Picard fixed-point theorem shows that the above iterative scheme converges to k_χ^∞ and that

$$\|k_\chi - k_\chi^\infty\|_\infty \le C\|k - k_\chi\|_\infty. \tag{2.18}$$

In other words, the smooth part of k_χ is well reconstructed provided that the non-smooth part $k - k_\chi$ of k is small. The result is not very satisfactory because the smallness hypotheses on k and σ depend on the norm of T^χ. In other words, the constraints of smallness on k and σ become exponentially stronger as the maximal wavenumber we want to reconstruct increases. Nonetheless, the result shows that reconstructions of optical parameters are indeed theoretically feasible from diffusion type measurements, but that problems are severely ill-posed.

3. Frequency modulation sources

We summarize here results obtained in [**9, 10, 11**]. Let $f(x)$ be the incoming boundary condition in (1.1) and $J(x) = \mathcal{D}^\omega f(x)$ be the measured current for $x \in \partial D$. Using the decomposition (2.2) and the definitions (2.5), we may define the Schwartz kernel $\mathbb{D}(x,y)$ of $\mathcal{D}$ such that

$$J(x) = \int_{\partial D} \mathbb{D}^\omega(x,y) f(y) dS(y).$$

The kernel $\mathbb{D}^\omega$ is a functional of the optical parameters $k(x,\kappa)$ and $\sigma(x)$. Experimental data for each source term $f(x)$ may be modeled as

$$J_E(x) = \int_{\partial D} \mathbb{D}^\omega_E(x,y) f(y) dS(y), \tag{3.1}$$

where $\mathbb{D}^\omega_E(x,y)$ would be the experimental linear operator mapping f to the possibly noisy outgoing measurements and $\mathbb{N}(x)$. The reconstruction of $k(x,\kappa)$ and $\sigma(x)$ could then be based on minimizing the error between the model and the experimental data and, for instance in a least squares formulation, finding $k(x,\kappa)$ and $\sigma(x)$ that minimize

$$\mathcal{F}(k,\sigma) := \frac{1}{2} \int_{\partial D^2} \left(\mathbb{D}^\omega - \mathbb{D}^\omega_E\right)^2 (x,y) dS(x) dS(y). \tag{3.2}$$

In practice, minimizations are based on a finite number of source terms f_q for $1 \leq q \leq Q$ and the functional may be modified as

$$\mathcal{F}_d(k,\sigma) := \frac{1}{2} \sum_{q=1}^{Q} \int_{\partial D} \left(\mathcal{D}^\omega f_q - z_q\right)^2 (x) dS(x), \tag{3.3}$$

where z_q is the experimental measurement corresponding to f_q, for instance $z_q(x) = \int_{\partial D} \mathbb{D}^\omega_E(x,y) f_q(y) dS(y)$ in the setting of (3.2). Because the measurements are now discrete, the reconstruction of the optical parameters from the measured data is under-determined. The parameters thus need be regularized.

Let us assume as in [**9, 10, 11**] that $k(x,\kappa) = k(x)\phi(\kappa)$ where $\phi(\kappa)$ is the Henyey-Greenstein phase function

$$\phi(\kappa) = \frac{1-g^2}{(1+g^2-2g\kappa)^{\frac{3}{2}}},$$

where $g \in [0,1)$ measures the degree of anisotropy ($g=0$ corresponds to isotropic scattering as in the preceding section) and is chosen as $g = 0.9$ in the two numerical simulations that follow. We thus wish to reconstruct $k(x)$ and $\sigma(x)$ from the available measurements. A possible regularization consists of assuming that k and σ are sufficiently smooth. We thus introduce the regularized functional

$$\mathcal{F}_d^\beta(k,\sigma) = \mathcal{D}_d(k,\sigma) + \beta\mathcal{I}(k,\sigma), \tag{3.4}$$

where the choice of $\mathcal{I}$ in [**10, 11**] is given by

$$\mathcal{I}(k,\sigma) = \frac{1}{2}\Big(\|k\|^2_{H^1(D)} + \|\sigma\|^2_{H^1(D)}\Big). \tag{3.5}$$

It remains to discretize the transport equation (1.1), here by a finite volume method, and minimize $\mathcal{F}_d^\beta$, based on the adjoint method and a limited memory BFGS algorithm [**11**]. The choice of the optimal β is based on the L-curve methodology; see [**11**]. Several numerical simulations are performed in the aforementioned references. Two interesting observations for us here are as follows.

Consider a two-dimensional computational domain $\bar{D} = [0,2]^2$ of size 2×2 cm^2 discretized with 80×80 uniform cells and a angular space $(0, 2\pi)$ uniformly discretized by 128 discrete directions. The transport equation (1.1) is used with the above discretization during the inversion process. The synthetic data z_q are constructed using a discretization twice as fine in all spatial and angular variables. We consider a setting with four sources located at the corners of the domain D and 20 detectors uniformly distributed over ∂D. The minimum of the functional (3.4) is sought by using a limited memory quasi-Newton iterative algorithm [**11**].

We consider a geometry with two small discs of radius 0.2 cm and centered at (1.35 cm, 1.35 cm) and (0.65 cm, 0.65 cm), respectively. The first disc is highly absorbing and the second one is highly scattering. Optical properties for the two discs are $\sigma_a = 0.2$ cm^{-1}, $\sigma_s = 70$ cm^{-1} and $\sigma_a = 0.1$ cm^{-1}, $\sigma_s = 80$ cm^{-1}, respectively. The background parameters are $\sigma_a = 0.1$ cm^{-1} and $\sigma_s = 70$ cm^{-1}. We present on top of Fig. 1 the reconstruction of both the absorption and scattering coefficients along the diagonal between $(0,0)$ and $(2,2)$ when $\omega = 0$. Notice the large cross-talk between the absorption and scattering reconstructions. The bottom row of Fig. 1 shows the same reconstruction for $\omega = 800$MHz.

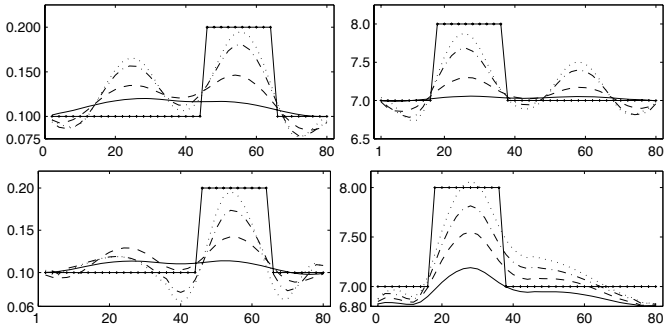

FIGURE 1. Reconstruction of the absorption coefficient (left) and scattering coefficient (right) along the diagonal between $(0,0)$ and $(2,2)$ after 40 (solid line), 80 (dashed line), 120 (dash-dotted line) and 156 (dotted line) iterations of the quasi-Newton algorithm at frequencies $\omega = 0$ (top) and $\omega = 0.8$GHz (bottom). The true piecewise constant coefficients are also indicated in solid lines.

Not only are the reconstructions more accurate, but the cross-talk between the reconstructions of the scattering and absorbing coefficients is significantly smaller. We refer the reader to [**11**] for a similar conclusion based on numerical simulations performed in three dimensions of space.

We now consider the three-dimensional reconstruction in [**11**], where D is a cylinder $D(0,1) \times (0,2)$ with $D(0,1)$ the two-dimensional disc of radius 1. Four sources are placed at $(\cos\theta, \sin\theta, 1)$ for $\theta = \frac{n\pi}{2}$, $n = 0,1,2,3$ and 32×7 detectors are placed at the surface of the cylinder at $(\cos\phi, \sin\phi, z_i)$ for 32 uniformly distributed angles ϕ and 7 uniformly distributed $z_i = \frac{i}{4}$, $1 \leq i \leq 7$. The background optical properties are $\sigma_a = 0.1$ cm^{-1} and $\sigma_s = 100$ cm^{-1}. A vertical cylindrical absorbing inclusion is placed inside the domain. The vertical cylinder is centered at $(0.5, 0, 1)$, has a radius of 0.2 and a vertical extension of 1.6.

Using the same minization procedure as in the previous numerical example, Fig.2 shows the error in the L^2 norm of the reconstructed absorption coefficient as a function of modulation frequency ω varying between 200MHz and 800MHz. We observe a steady decrease in the error as frequency increase from a relative error of 9% when $\omega = 200$MHz to an error of 6% when $\omega = 800$MHz.

These two numerical simulations support the following conclusion: larger values of ω allow us to obtain better reconstructions of the optical parameters $k(x)$ and $\sigma_s(x)$.

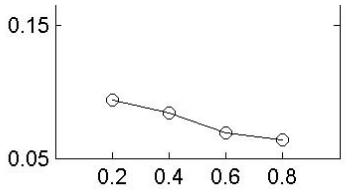

FIGURE 2. Relative L^2 error of the reconstructed absorption coefficient in the aforementioned three-dimensional simulation as a function of modulation frequency ω.

4. High modulation frequency asymptotics

In this section, we propose a theoretical explanation for the behavior presented in the preceding section. We show that, as ω increases, the contributions of scattering in the diffusion-type measurements decreases. More specifically, in two dimensions of space, we show that the amplitude of the contribution of the ballistic part in the measured data $\mathcal{D}^\omega$ is independent of modulation frequency ω; the amplitude of the single scattering contribution in $\mathcal{D}^\omega$ is at most of order $\omega^{-\frac{1}{2}}$, and the contribution of the higher orders of scattering in $\mathcal{D}^\omega$ is negligible compared to $\omega^{-\frac{1}{2}}$. The details of the study will appear in a joint work with Ian Langmore [**2**].

Let us come back to the definitions (2.5) and (2.6). When $\omega \neq 0$, $E(x,y)$ should be replaced in those definitions by

$$E^\omega(x,y) = e^{i\omega|x-y|}E(x,y), \tag{4.1}$$

since the absorption term $\sigma(x)$ is replaced by $\sigma(x)+i\omega$; $E^\omega(x_1,\ldots,x_n)$ is defined by modifying (2.4) accordingly. We define the operators $T_m^\omega(k)$ for $m \geq 0$ as in (2.5) with E replaced by E^ω and the measurements $\mathcal{M}^\omega(f,g)$ in (2.2) accordingly. We then formally obtain that

$$\mathcal{M}^\omega(\delta_{x_0},\delta_x) = \mathcal{D}^\omega[\delta_{x_0}](x) = \sum_{m=0}^{\infty} T_m^\omega(x_0,x). \tag{4.2}$$

We assume that we have access to these measurements for all x_0 and x at the domain's boundary ∂D. The intensity of the ballistic part is not affected by the modulation frequency, for

$$T_0^\omega(x_0,x) = e^{i\omega|x-x_0|}T_0(x_0,x). \tag{4.3}$$

Let us now turn to the scattering contributions. We assume here that D is a domain with real-analytic boundary ∂D (for instance D is a disc). We also assume that scattering takes the form $k(x)\phi(\kappa)$ and that $k(x)$

vanishes in the $0 < \delta$-vicinity of the boundary ∂D. Then the single scattering term T_1^ω may be shown to be given by

$$\begin{aligned} T_1^\omega(x_0,x) &= \int_{\mathbb{R}}\int_0^{2\pi} F(t,\theta)e^{i\omega\varphi_t(\theta)}dtd\theta, \\ F(t,\theta) &= k(x_0+tv)\phi(v\cdot w)E(x_0,x_0+tv,x)|\nu_x\cdot w|, \\ \varphi_t(\theta) &= t+|x-(x_0+tv)|, \\ v &= v(\theta)=(\cos\theta,\sin\theta) \\ w &= w(t,\theta)=\tfrac{x-(x_0+tv)}{|x-(x_0+tv)|}. \end{aligned} \tag{4.4}$$

The single scattering contribution may thus be seen as an oscillatory integral with (smooth) amplitude $F(t,\theta)$ and highly oscillatory phase $\omega\varphi_t(\theta)$. It turns out that for each fixed value of t, the phase $\varphi_t(\theta)$ admits a unique critical point corresponding to θ given by $(\cos\theta,\sin\theta) = v = \frac{x-x_0}{|x-x_0|}$. Most of the energy in $T_1^\omega(x_0,x)$ is thus concentrated on single scattering events occurring along the segment $[x_0,x]$.

More precisely, a careful stationary phase analysis shows that

$$\begin{aligned} T_1^\omega k(x_0,x) = \frac{e^{i\omega|x-x_0|}}{\sqrt{\omega}}\sqrt{\pi}e^{i\frac{\pi}{4}}E(x_0,x)|\nu_x\cdot v|\times \\ \int_0^{|x-x_0|} k(x_0+tv)\phi(1)\sqrt{\frac{|x-x_0|-t}{t|x-x_0|}}dt + O(\frac{1}{\omega^{\frac{3}{2}}}), \end{aligned} \tag{4.5}$$

where $v=\frac{x-x_0}{|x-x_0|}$, and where the remainder is uniform in x_0 and x.

Similar stationary phase analyses show that the higher-order contributions are even smaller. More precisely, we may show that

$$|T_m^\omega(k)(x_0,x)| \leq \frac{C_s}{\omega^s}\rho^m, \tag{4.6}$$

where $\rho < 1$ for $\|k\|_\infty$ sufficiently small and where C_s is a constant independent of ω, x_0, and x for $\frac{1}{2} < s < \frac{2}{3}$. This shows that

$$\mathcal{M}^\omega(\delta_{x_0},\delta_x) = e^{i\omega|x-x_0|}\Big(M_0(x_0,x)+\frac{M_1(x_0,x)}{\sqrt{\omega}}\Big)+O(\omega^{-\frac{2}{3}+\eta})\Big), \tag{4.7}$$

for all $\eta > 0$, where, still with $v=\frac{x-x_0}{|x-x_0|}$,

$$\begin{aligned} M_0(x_0,x) &= T_0(x_0,x) = \frac{E(x_0,x)|\nu_x\cdot v||\nu_{x_0}\cdot v|}{|x_0-x|^{n-1}} \\ M_1(x_0,x) &= \sqrt{\pi}e^{i\frac{\pi}{4}}E(x_0,x)|\nu_x\cdot v|\times \\ &\qquad \int_0^{|x-x_0|} k(x_0+tv)\phi(1)\sqrt{\frac{|x-x_0|-t}{t|x-x_0|}}dt. \end{aligned} \tag{4.8}$$

If we have access to $\mathcal{M}^\omega(\delta_{x_0}, \delta_x)$ for a large value of ω and for all x_0 and x, then we measure $E(x_0, x)$ up to an error of size $\omega^{-\frac{1}{2}}$. Upon talking the logarithm, this gives us access to the line integral of $\sigma(y)$ along the segment $[x, x_0]$. We thus obtain the Radon transform of $\sigma(y)$, which may be inverted explicitly to provide an explicit expression for the total attenuation parameter $\sigma(x)$.

Let us now assume that we have access to $\mathcal{M}^{\omega_k}(\delta_{x_0}, \delta_x)$ for two large modulation frequencies $\omega_1 > \omega_2 \gg 1$. Then we have access to $\alpha_k = e^{-i\omega_k|x-x_0|}\mathcal{M}^{\omega_k}(\delta_{x_0}, \delta_x)$ for all x_0 and x and find that

$$\begin{aligned} M_0 &= \frac{\sqrt{\omega_1}\alpha_1 - \sqrt{\omega_2}\alpha_2}{\sqrt{\omega_1} - \sqrt{\omega_2}} + O(\omega_2^{-\frac{2}{3}+\eta}) \\ M_1 &= \Big(\frac{1}{\sqrt{\omega_2}} - \frac{1}{\sqrt{\omega_1}}\Big)^{-1}(\alpha_2 - \alpha_1) + O(\omega_2^{\frac{-2}{3}+\frac{1}{2}+\eta}). \end{aligned}$$

We may then reconstruct $\sigma(x)$ from knowledge of M_0 as before, which provides us with knowledge of

$$R_1 k(x_0, x) = \int_0^{|x-x_0|} k(x_0 + tv)\sqrt{\frac{|x-x_0| - t}{t|x-x_0|}}dt, \qquad (4.9)$$

provided that the anisotropy factor in the forward direction $\phi(1)$ is known. We observe that $R_1 k(x_0, x)$ is a weighted Radon transform of k along the segment (x_0, x). Because we have assumed that k was supported away from ∂D, we observe that the weight $w(x, x_0, t) = \sqrt{\frac{|x-x_0|-t}{t|x-x_0|}}$ is real-analytic in t, x, and x_0, on the support of k. We can then use the general results in [**6**] to obtain that R_1 is an injective transform so that k is uniquely determined by $R_1 k$ and that the reconstruction is mildly ill-posed (with Hölder-type stability).

These results show that $\mathcal{D}^\omega$ known for two frequencies $\omega_1 > \omega_2$ uniquely determines the weighted Radon transforms of $k(x)\phi(1)$ and $\sigma(x)$ up to error terms of order $\omega_2^{-\frac{2}{3}+\frac{1}{2}+\eta}$. Provided that $\phi(\kappa)$ is known in advance, we thus obtain the approximate reconstruction of $\sigma(x)$ and $k(x)$ from knowledge of two modulation frequency measurements $\mathcal{D}^\omega$. Moreover, unlike the case $\omega = 0$, the reconstructions are based on inverse Radon transforms, which are mildly ill-posed rather than severely ill-posed as in section 2. To some extent, the large-ω behavior of $\mathcal{D}^\omega$ explains the results obtained in section 3: as ω increases, the effects of (total) absorption and scattering separate, which explains why both optical parameters can be reconstructed in a more stable fashion.

5. Conclusions

This short review paper supports the following conclusions. Inverse transport problems based on knowledge of $\mathcal{D}$ yield severely ill-posed as for the diffusion equation. This means that the backward map from the data to the optical parameters is more unstable than any finite number of differentiations. Noise is very much amplified during the inversion procedure and we should therefore not expect to obtain too fine a resolution.

Two possible solutions that allow us to obtain more accurate reconstruction are as follows. One may either look for angularly resolved data, which gives an approximation of the albedo operator $\mathcal{A}$. The reconstructions of the optical parameters have been show to be Hölder stable (the map from the data back to the optical parameters is not more singular than a finite number of differentiations) in several cases. When such angularly resolved measurements are not accessible, an alternative strategy would be to increase the modulation frequency ω. Stationary-phase-type expansions show that the reconstruction of $k(x)$ and $\sigma(x)$ is feasible with Hölder-type stability provided that $\mathcal{D}^\omega$ is available for two large frequencies $\omega_1 \neq \omega_2$.

One of the main drawbacks of the asymptotic expansions performed in section 4 is that ω needs to be on the order of 100GHz in order for the large-ω assumptions to make sense for domains of width equal to 10cm. Such modulations seem to be much larger than what is technologically feasible at present. Note that high modulation frequencies correspond to short time scales and thus accurate sampling in the time domain. High modulation frequencies are thus very similar to accurate measurements in the time domain, where first arrivals, which correspond to ballistic particles, are just followed by particles that scatter once, whereas multiply scattered particles arrive at somewhat later times. Similar small-time asymptotic expansions could then be performed as was done in section 4, with the same conclusion that time-dependent angularly-averaged measurements allow for Hölder stable reconstructions of the optical parameters as well.

Acknowledgment

The author would like to thank A. Hielscher, I. Langmore, F. Monard, and K. Ren for many fruitful discussions and collaborations on inverse transport theory and its applications to optical tomography. This work was supported in part by NSF Grants DMS-0239097 and DMS-0554097.

References

[1] S. R. Arridge, *Optical tomography in medical imaging*, Inverse Problems **15** (1999), R41–R93.

[2] G. Bal and I. Langmore, *Inverse transport with large modulation frequencies*, preprint (2008).

[3] G. Bal, I. Langmore, and F. Monard, *Inverse transport with isotropic sources and angularly averaged measurements*, submitted (2008).

[4] A.P. Calderón, *On an inverse boundary value problem*, Seminar on Numerical Analysis and its Applications to Continuum Physics, Soc. Brasileira de Matematica, Rio de Janeiro (1980), 65–73.

[5] R. Dautray and J.-L. Lions, *Mathematical Analysis and Numerical Methods for Science and Technology. Vol.6*, Springer Verlag, Berlin, 1993.

[6] B. Frigyik, P. Stefanov, and G. Uhlmann, *The x-ray transform for a generic family of curves and weights*, prepring (2008).

[7] I. Langmore, *The stationary transport equation with angularly averaged measurements*, submitted (2007).

[8] M. Mokhtar-Kharroubi, *Mathematical Topics in Neutron Transport Theory*, World Scientific, Singapore, 1997.

[9] K. Ren, G. S. Abdoulaev, G. Bal, and A. H. Hielscher, *Algorithm for solving the equation of radiative transfer in the frequency domain*, Optics Letter **29(6)** (2004), 578–580.

[10] K. Ren, G. Bal, and A. H. Hielscher, *Frequency domain optical tomography based on the equation of radiative transfer*, SIAM J. Sci. Comput. **28** (2006), 1463–1489.

[11] ———, *Transport- and diffusion-based optical tomography in small domains: A comparative study*, Appl. Optics (2007).

[12] P. Stefanov, *Inside out: Inverse problems and applications*, MSRI publications, vol. 47, ch. Inverse Problems in Transport Theory, Cambridge University Press, Cambridge, UK, 2003.

[13] G. Uhlmann, *Developments in inverse problems since Calderón's foundational paper*, Harmonic analysis and partial differential equations, Chicago Lectures in Math., Univ. Chicago Press, Chicago, IL (1999), 295–345.

DEPARTMENT OF APPLIED PHYSICS & APPLIED MATHEMATICS, COLUMBIA UNIVERSITY, NEW YORK, NY 10069

E-mail address: gb2030@columbia.edu